

## Evolution of magnetic response as a function of annealing temperature in Fe-based alloys

Damián Gargicevich<sup>1</sup>, Federico Guillermo Bonifacich<sup>1</sup>,  
Osvaldo Agustín Lambri<sup>1</sup>, Pablo Chiappero<sup>1</sup>, José Ángel Cano<sup>1</sup>,  
Griselda Irene Zelada<sup>1</sup>, José Ignacio Pérez-Landazábal<sup>2,3</sup>,  
Vicente Recarte<sup>2,3</sup>, Víctor Martín Galván Josa<sup>4</sup>,  
María Cecilia Blanco<sup>5</sup>, Gabriel Julio Cuello<sup>6</sup>

<sup>1</sup> CONICET-UNR, Laboratorio de Materiales, Escuela de Ingeniería Eléctrica, Centro de Tecnología e Investigación Eléctrica, Facultad de Ciencias Exactas, Ingeniería y Agrimensura, Av. Pellegrini 250, 2000, Rosario, Santa Fe, Argentina.

e-mail: [gargi@fceia.unr.edu.ar](mailto:gargi@fceia.unr.edu.ar); [bonifaci@fceia.unr.edu.ar](mailto:bonifaci@fceia.unr.edu.ar); [olambri@fceia.unr.edu.ar](mailto:olambri@fceia.unr.edu.ar); [pjchiappero@gmail.com](mailto:pjchiappero@gmail.com); [jacano@fceia.unr.edu.ar](mailto:jacano@fceia.unr.edu.ar); [gizelada@fceia.unr.edu.ar](mailto:gizelada@fceia.unr.edu.ar);

<sup>2</sup> Departamento de Física, Universidad Pública de Navarra, Pamplona, España.

<sup>3</sup> Instituto de Materiales Avanzados (INAMAT), Universidad Pública de Navarra, Campus de Arrosadía s/n, 31006 Pamplona, Navarra, España.

e-mail: [ipzlanda@unavarra.es](mailto:ipzlanda@unavarra.es); [recarte@unavarra.es](mailto:recarte@unavarra.es)

<sup>4</sup> CONICET-UNC, Facultad de Matemática, Astronomía y Física, Universidad Nacional de Córdoba, Medina Allende, Ciudad Universitaria, 5000, Córdoba, Córdoba, Argentina.

e-mail: [galvan@famaf.unc.edu.ar](mailto:galvan@famaf.unc.edu.ar)

<sup>5</sup> CONICET-UNC, Facultad de Ciencias Químicas, Universidad Nacional de Córdoba, Av. Haya de la Torre, Ciudad Universitaria, 5000, Córdoba, Córdoba, Argentina.

e-mail: [ceciliablanca3@gmail.com](mailto:ceciliablanca3@gmail.com)

<sup>6</sup> Instituto Laue-Langevin, 71, Av. des Martyrs, 38042, Grenoble, Isère, France.

e-mail: [cuello@ill.eu](mailto:cuello@ill.eu)

---

### ABSTRACT

The magnetic response, coercive force and magnetic induction, in Fe-10at.% Si, Fe-6at.% Al-9at.% Si and Fe-4at.% Al-8at.% Ge alloys as a function of the annealing temperature was determined and correlated to the microstructural state. The microstructural characterization was made through differential thermal analysis, mechanical spectroscopy and neutron thermodiffraction studies. It has been determined that the increase in the order degree and the decrease in the mobility of structural defects lead to a deterioration of the magnetic quality of the alloys above detailed.

**Keywords:** Fe-based alloys, microstructure, Improvement of magnetic properties, Hysteresis loops

---

### 1. INTRODUCTION

Fe-based alloys are often used as magnetic cores, which has a particular importance in energy conversion and transport, high frequency applications, magnetic recording, choke, inductors, etc. [1–4]. The study of the magnetic properties and its optimization plays a crucial role in the electric industry. In fact, it is known that order and recovery has a strong influence on the magnetic properties [1–3]. However, despite the spread technological use of magnetic alloys there is scarce bibliography about the relation between microstructure and magnetic behaviour.

In the present work, differential thermal analysis, mechanical spectroscopy and neutron thermodiffraction studies were performed to reveal the state of the microstructure. These studies were related to the characteristic parameters for describing the hysteresis loops; as coercive force and maximum induction reached at a given fixed field. The magnetic quality of the material is explained on the basis of the mobility of the domain walls controlled by the interaction with defects. Indeed, the great importance of the first part of the magnetization process before reaching the saturation elbow, which is utilized as working point in electrical machines, is well known [3,4]. Therefore, the study of the mobility of the domain walls controlled

by the microstructure arises as a critical technological issue [3,4].

## 2. MATERIALS AND METHODS

Studied samples were polycrystals both commercial and laboratory prepared, of compositions: Fe-10at.% Si Fe-6at.% Al-9at.% Si and Fe-4at.% Al-8at.% Ge. Fe-10at.% Si were commercial samples provided by NKK Corp. Samples were homogenized at 1323 K during 1 hour under high vacuum and quenched in room temperature (RT) water.

Microstructure was analyzed by means of differential thermal analysis (DTA), mechanical spectroscopy (MS) and Neutron thermodiffraction (ND) studies.

DTA measurements were performed in a conventional differential calorimeter assembled at the Laboratory with stainless steel crucibles under pure Argon atmosphere at normal pressure. The heating rate was 5°/minute and it was controlled by a Lake Shore DRC-91C device.

Mechanical spectroscopy measurements were performed in an inverted torsion pendulum at frequencies close to 1 Hz in free decaying vibrations [5]. Measurements have been performed under vacuum (about  $10^{-5}$  Pa). The employed samples were bars of rectangular section (1 mm×2.2 mm×20 mm). The maximum strain on the surface of the sample was  $5 \times 10^{-5}$ . Damping ( $Q^{-1}$ ) and square frequency (which is proportional to the shear modulus), were measured with an error less than 2%. The measurements were carried out during subsequent heating and cooling runs on the same specimen. A heating and its cooling run is hereafter called a thermal cycle. The heating rate was 1.5 K/min.

Neutron powder diffraction studies were performed at D20 and D1B installations in the Institute Laue-Langevin (ILL), Grenoble, France. In situ experiments at D20 were performed during heating from RT up to 1050 K and from RT up to 1300 K, for Iron Silicon and Fe-Al-Ge alloys, respectively. Measurements were performed under high vacuum ( $10^{-2}$  Pa). The neutron wavelength was  $\lambda = 1.3\text{Å}$ . The heating rate was 4 K/min. In addition, neutron thermodiffraction studies for Fe-Al-Si were performed at D1B. The used neutron wavelength was  $\lambda = 1.28\text{Å}$ . Spectra were obtained under high vacuum ( $10^{-2}$  Pa) from RT up to 1173 K. The heating rate was 3 K/min.

Magnetic cycles were recorded at RT in a Laboratory assembled automatic loop tracer. Magnetic field was generated by a 3000 winding coil connected to an analogical wave generator Protek B-801 and a digital oscilloscope Rigol DS1052E used for data acquisition. The average of 5 cycles was considered for each measurement. Samples for magnetic loops were thermally treated step by step by increasing the temperature in 50 K, starting from RT up to 1123 K, under high vacuum. The heating rate was of 1.5 K/min and the cooling was without furnace under high vacuum.

## 3 RESULTS AND DISCUSSION

### 3.1 Differential thermal analysis

Figure 1 shows the DTA thermogram measured in an as-quenched Fe-10at.% Si sample (blue circles), from where three exothermic reactions at around 560 K, 640 K and 800 K can be observed. In addition, the change in base line related to the Curie temperature can be also observed to appear at around 973 K. The first exothermic reaction at around 550 K was already related to increase in the degree of B2 order reached by the quenching process [6].

In addition, the exothermic peaks at around 640 K and 800 K were already related to the recovery of vacancies and the recovery of the structure, respectively. In fact, at around 600 K in high purity iron the total recovery of the excess of vacancies out of the equilibrium has been determined from positron annihilation spectroscopy [7–9]. Besides, a temperature of 800 K is in agreement with the temperature of recovery and recrystallization for iron [10,11].

The thermogram for an as-quenched Fe-6at.% Al-9at.% Si sample (red squares) is also shown in Figure 1. It can be observed a clear exothermic reaction at around 650 K and subsequently at higher temperatures the change in baseline related to the Curie temperature at around 980 K appears. At the same temperature the  $DO_3 \rightarrow bcc$  transition develops, according to phase diagram [12,13].

The thermal reaction at lower temperature can be related to both the increase of the  $DO_3$  order after the quenching process, in agreement with previous works [14], and to the recovery of vacancies [7–9]. In fact, the reaction peak is wide enough for involving a superposition of reaction processes.

The thermal behaviour for Fe-4at.% Al-8at.% Ge is shown in Figure 1 by means of green triangles. It

can be seen a wide exothermic peak (two stage peak) between around 500 K and 673 K which can be related to the recovery of quenched-in-vacancies, in agreement with the Fe-10at.% Si and Fe-6at.% Al-9at.% Si alloys and previous works [7–9]. The peak at higher temperatures of around 850 K, which can be observed partially from 700 K onwards, can be related to the recovery and recrystallization of the structure [10,11].

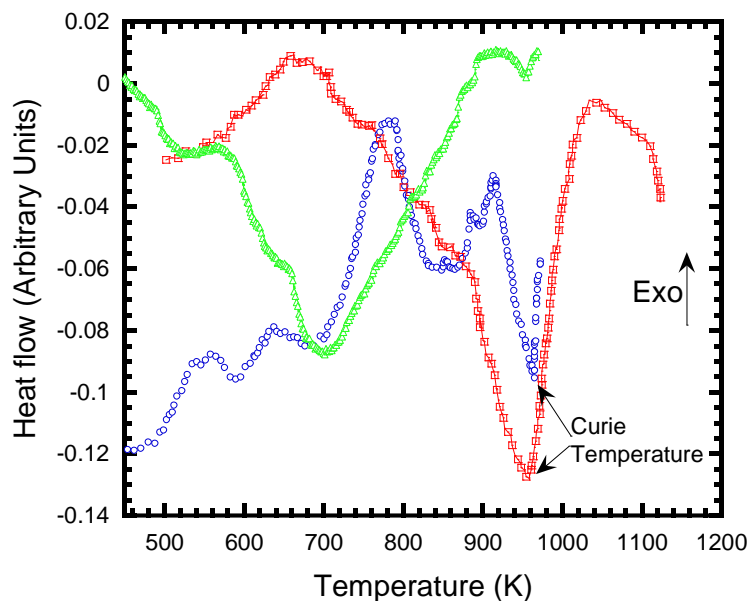


**Figure 1:** DTA thermograms for Fe-10at% Si (blue circles), Fe-6at.% Al-9at.% Si (red squares), Fe-4at.% Al-8at.% Ge (green triangles). Not all measured points are shown for clarity.

### 3.2 Neutron thermodiffraction

Neutron thermodiffraction studies performed in the Fe-10at.% Si samples, determined that the as-quenched sample has an ordered B2 structure and during its warming the alloy exhibits the B2 → bcc transformation at 973 K; according to the phase diagram [6], see Figure 2. In addition, during the cooling the B2 order restores at the same temperature. Moreover, the order degree after a warming to 1050 K has increased, Figure 2

[6]. D0<sub>3</sub> structure has never been observed from neutron patterns [6].

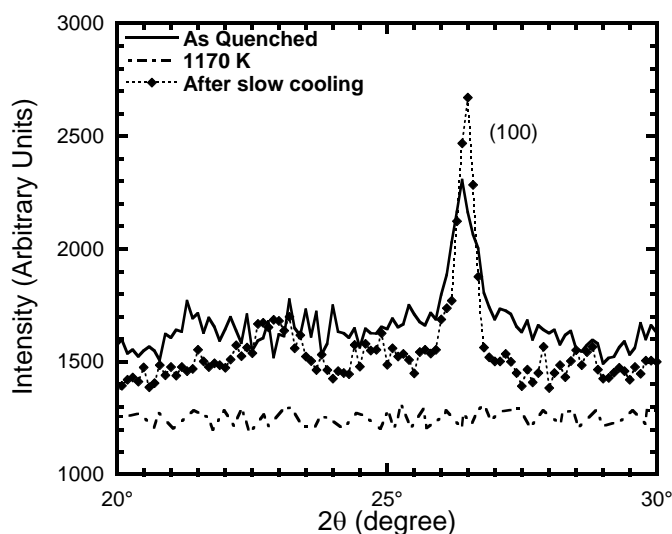


**Figure 2:** Neutron diffraction patterns for three different temperatures for Fe-10at.% Si.

Neutron thermodiffraction studies in as-quenched Fe-6at.% Al-9at.% Si sample, determined the appearance of D0<sub>3</sub> order at room temperature. Above 983 K, the order disappears, as shown by the disappearance of the (1 1 1) and (2 0 0) reflections related to the D0<sub>3</sub> structure, Figure 3 [12,15]. In addition,

during the cooling, after a previous heating up to 1150 K, the order is restored approximately at the same temperature (983 K) [12].

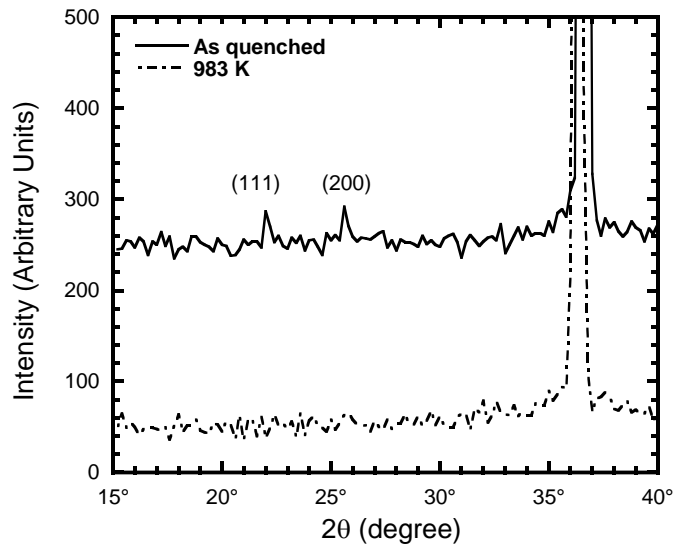


**Figure 3:** Neutron diffraction patterns for Fe-6at.% Al-9at.% Si at different temperatures.

Neutron thermodiffraction studies for Fe-4at.% Al-8at.% Ge have shown that this alloy is disordered in  $\alpha$  phase in the whole explored temperature range, between room temperature and 1300 K, see Figure 4.

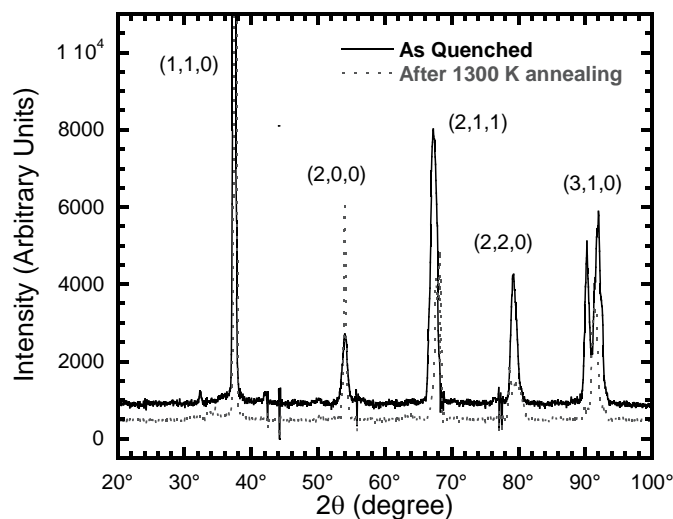


**Figure 4:** Neutron thermodiffraction pattern for Fe-4at.% Al-8at.% Ge.

### 3.3 Mechanical spectroscopy

In order to determine the effects of the microstructural changes above described on the mechanical behaviour, mechanical spectroscopy studies were performed. Figure 5 show the damping and modulus behaviour measured during warming as a function of temperature during successive thermal cycles performed up to different maximum temperatures for Fe-10at.% Si. All spectra show the characteristic grain boundary relaxation peak (GB), around 800 K [6,16]. The peak temperature of the maximum related to GB moves towards higher temperatures during the cycles up to 973 K. In the second heating the shift is very small, being larger during the third run up in temperature. In contrast, when the sample was previously measured up to 1050 K, the peak temperature of the maximum during the heating run is shifted towards smaller temperatures (black diamond). Besides this, the peak temperature is very close to the initial peak

temperature corresponding to the as-quenched sample. Nevertheless, the damping spectrum changes strongly when the sample was thermally treated up to 1273 K [6,17].

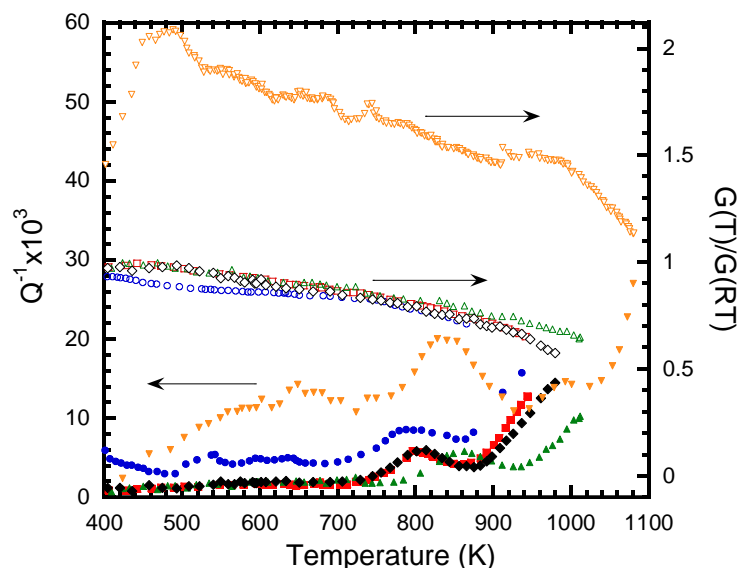


**Figure 5:** Damping ( $Q^{-1}$ ), full symbols, and normalized shear modulus ( $G(T)/G(RT)$ ), empty symbols, as a function of temperature for Fe-10at.% Si alloy. Blue circles, as-quenched sample; red squares, after heating to 973 K; green triangles, after two heating to 973 K; black diamonds, after heating to 1050 K; orange inverted triangles, after a heating to 1273 K. Only some measured points were plotted for clarity.

During the recovery of the structure above 800 K, some dislocations move to the grain boundaries reducing their mobility, leading to the small increase of the 800 K peak temperature in the second warming run, red squares in Figure 5. In fact, the increase of the order degree after reaching 973 K produces an increase of internal stresses generated by the reorganization of defects in the ordered B2 phase. In particular dislocation must move in pairs towards the grain boundary where they are locked, reducing the grain boundary mobility [6]. In addition, the increase in the modulus values shown in Figure 5 for the second and subsequent warming runs is in agreement with the recovery process and with the assumption of an increase of internal stress developed by the dissociation of superdislocations in the B2 superlattice obtained during cooling.

During heating up to 1050 K the sample transforms according to the phase diagram. The B2 phase transforms to a bcc at 973 K and for higher temperatures the sample is disordered and the super dislocations disappear. Then, the structure can recover quenched-in-defects, which were retained in the ordered B2 superlattice. This effect leads to shift the peak temperature of GB towards smaller temperature. Besides, a thermal treatment at temperatures above 1273 K removes more quenched-in-dislocations associated to grain boundaries thus improving the mobility of grain boundaries and consequently increasing the GB peak height. The large modulus increases in the second heating run for the sample slow cooled from 1273 K agrees with a better reorganization of the dislocation structure.

The behaviour of the modulus as the function of temperature is shown through the behaviour of the ratio  $G(T)/G(RT)$ , where  $G(RT)$  is the shear modulus at room temperature, as a function of temperature. The first increase in the modulus between 400 K and 500 K can be related to an interaction process between point defects and dislocations.

Figure 6 shows the damping spectra measured up to 1130 K (left axis) for a Fe-6at.% Al-9at.% Si sample for two subsequent thermal cycles. The damping change between 700 K and 1000 K is small ( $Q^{-1} \sim 2 \times 10^{-3}$ ) but the damping increases strongly up to values  $Q^{-1}$  of about  $110 \times 10^{-3}$  for higher temperatures. During the subsequent cooling run a damping peak develops. A thermal hysteresis in the damping of about 100 K appears in the temperature interval 850 – 1050 K. Besides, the elastic modulus (ratio  $G(T)/G(RT)$ ) exhibited a hysteretic behaviour in the same temperature range, see right axis in Figure 6. The modulus values during the cooling runs were smaller than during the heating runs.

As it was already pointed out in Ref. [12] the Fe-6at.% Al-9at.% Si sample is  $D0_3$  ordered at room temperature, Figure 3. However, at temperatures close to 983 K, the  $D0_3$  structure changes to bcc in

agreement with the ternary phase diagram [13]. This temperature is close to the one where the damping starts to increase strongly (980 K). Moreover, the temperature where the strong increase in the damping appears does not shift towards higher temperatures when the vibration frequency is increased. This kind of behaviour is the usual one for a phase transition process [19], in agreement with the neutron diffraction results and phase diagram. As in previous studied cases, after the  $DO_3 \rightarrow bcc$  transition, the order degree is reduced and then the mobility of dislocations and grain boundaries is enhanced, leading to a recovery of the microstructure. Consequently, again the GB relaxation peak appears during the cooling process. The temperature of this peak is also close to the solute peak for iron [6,11,12].

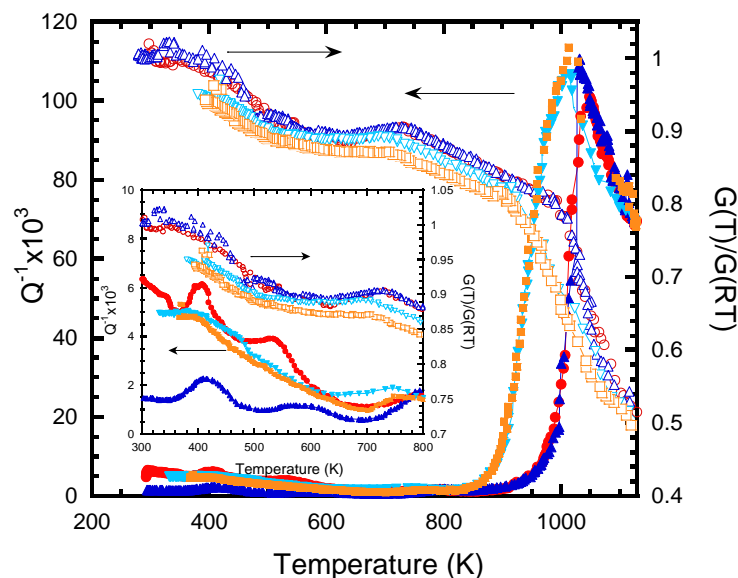


**Figure 6:** Damping ( $Q^{-1}$ ), full symbols, and normalized shear modulus ( $G(T)/G(RT)$ ), empty symbols, as a function of temperature. Blue triangles, heating first thermal cycle; inverted light blue triangles, cooling first thermal cycle; red circles, heating second thermal cycle; orange squares, cooling second thermal cycle. Inset shows a zoom of low temperature spectra.

Returning to the influence of the thermal cycles on the mechanical spectroscopy response, it can be seen that, the thermal cycles lead to an increase in the damping values in the temperature interval from room temperature up to around 700 K, see Figure 6. It indicates that some recovery of the microstructure has taken place, due to the increase in the magneto-mechanical damping contribution.

Besides this, the damping and the modulus curves during the subsequent thermal cycles up to 1130 K are not modified. Moreover, by increasing the final temperature of the thermal cycles up to 1200 K does not modify the damping and modulus behaviours.

Figure 7 shows the behaviour of both the damping and modulus as a function of temperature for a Fe-4at.% Al-8at.% Ge alloy. As it can be seen from the Figure during the first run up in temperature the damping slightly decreases up to around 620 K, followed by an increase in the damping values from 620 K onwards. Moreover, the GB peak can be observed at around 800 K. In addition, the modulus exhibit firstly an increase from around 400 K up to around 600 K, followed by a decrease as the temperature increases. The decrease in damping values and the increase in the modulus up to a temperature of around 600 K is similar to the exhibited by Fe-10at.% Si and it can be related to the pinning of dislocations for point defects. However, the decrease in the damping values between 400 K and around 600 K can take a contribution from the magneto-mechanical contribution.

During the second warming in the second thermal cycle the damping values in the temperature range between 400 K and around 650 K increase, exhibiting the appearance of a damping peak at around 570 K which can be related to the interaction of defects with dislocations. Moreover, the height of the grain boundary peak has increased as a consequence of the recovery of the structure over 873 K (see Figure 1). The recovery of the microstructure remove quenched-in-defects and -dislocations located at the grain boundaries and then the mobility of GB is increase giving rise to the increase in the GB peak height. In addition, after the development of the recovery, the reorganization of the microstructure is revealed by the more monotonously

decrease of the modulus values as the temperature is increased.

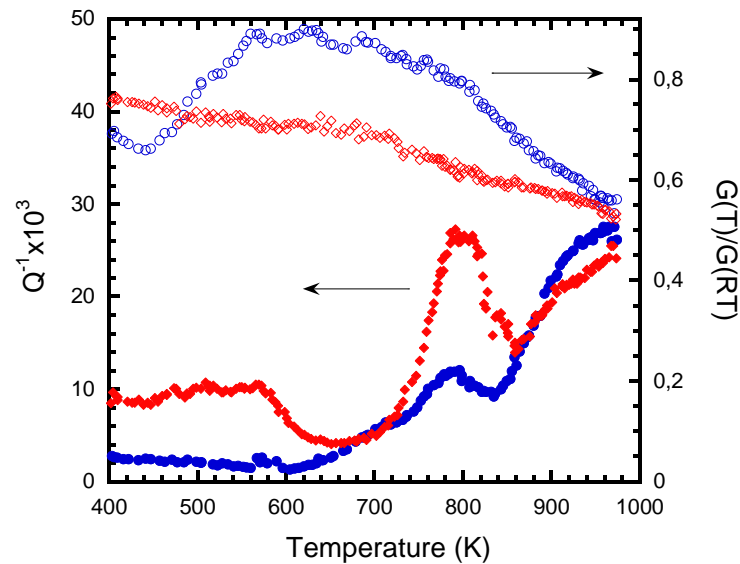


**Figure 7:** Damping ( $Q^{-1}$ ), full symbols, and normalized shear modulus ( $G(T)/G(RT)$ ), empty symbols, as a function of temperature for Fe-4at.% Al-8at.% Ge. Blue circles, heating first thermal cycle; red diamonds, heating second thermal cycle. Only half points are shown for clarity.

### 3.4 Hysteresis loops

Figure 8 shows the behaviour of the value of the magnetic induction at the tips,  $B_m$ , corresponding to  $H = 150$  A/winding and the coercive force,  $H_c$ , as a function of the annealing temperature. As it can be seen from the Figure  $B_m$  and  $H_c$  do not exhibit a monotonous behaviour as a function of annealing time, allowing us to separate the curves in four zones as the temperature increases.

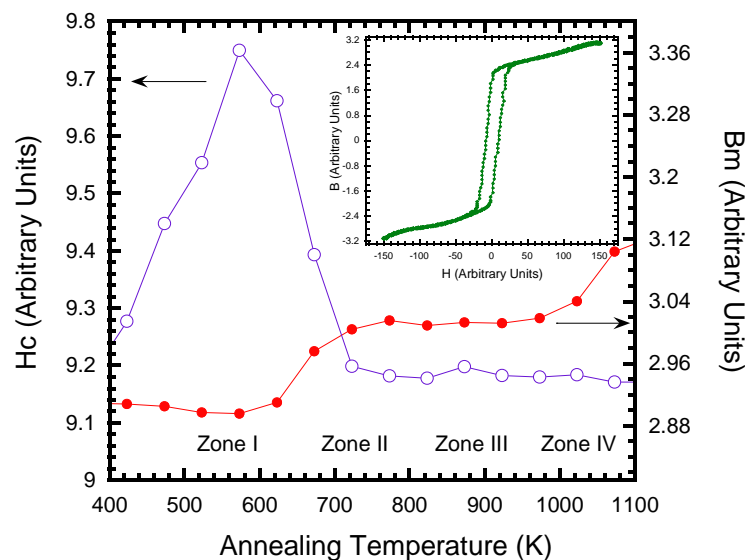


**Figure 8:**  $B_m$  and  $H_c$  as a function of annealing temperature for Fe-10at.% Si. Magnetic loops were traced at RT. Inset shows a hysteresis loop.

Therefore, paying attention to the microstructural evolution above described, we can explain the behaviour of  $B_m$  and  $H_c$  in each one of the temperature intervals detailed in Figure 8. Indeed, the behaviour of  $B_m$  and  $H_c$  in zone I can be related to the increase of the order degree promoted by the temperature increases (see Figure 1) and also for the pinning of dislocations (see Figure 5). The increase of internal



stresses leads to a decrease in the mobility of the domains walls through a magnetostrictive coupling, reducing Bm and increasing Hc.

In zone II, the start of the GB movement is occurring, due to the start of the low temperature tail of GB peak, so dislocations at the grain boundaries and grain boundary increase their mobility, Figure 5; allowing a rearrangement of the microstructure. Then, the rearrangement of the microstructure, in order to decrease the free energy by heating, leads to a decrease in the amount of blocking defects which improves the mobility of domains walls; leading to an increase in Bm and a decrease in Hc.

In zone III, Bm and Hc behave almost constant which could be controlled by the competence of both the order increase and the further recovery of the structure; as the annealing temperature increases.

Finally, in zone IV, above the B2 → bcc transformation at 973 K which allows a larger recovery of the structure due to the superdislocations vanish; Bm and Hc increases and decreases, respectively; as a consequence of an improvement in the mobility of the domains walls. Indeed, the decrease in the amount of quenched-in-defects and -dislocations, after the heating at temperatures over the B2 → bcc transformation, leads to an improvement of the magnetic quality, since the mobility of domains walls has increased because the less amount of obstacles interacting through a magnetostrictive phenomenon.

It should be highlighted that, as the magnetic loops are recorded at room temperature, the improvement of the magnetic quality after annealing temperatures over the B2 → bcc transformation, is controlled mainly by the recovery of defects and not by the B2 order degree, because the order state have reached already its maximum value. This is in agreement with several works, which not report a deterioration of the magnetic quality by the appearance of B2 order [20,21]. In contrast, the deterioration of magnetic quality was reported to appear with the development of D0<sub>3</sub> superstructure [20,21]. Therefore, in Fe-10at.% Si alloys the magnetic quality is mainly controlled by the recovery of defects, being the B2 ordering a less important contribution.

Figure 9 shows the behaviour of Bm and Hc for the ternary Fe-6at.% Al-9at.% Si as a function of temperature, where three zones of different monotony can be chosen.

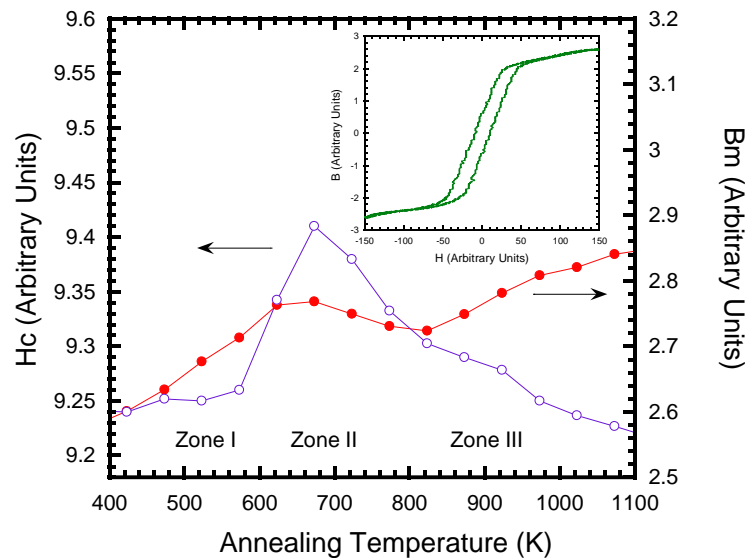


**Figure 9:** Bm and Hc as a function of annealing temperature for Fe-6at.% Al-9at.% Si. Being magnetic loops traced at room temperature. Inset shows a hysteresis loop.

The behaviour of Bm and Hc in zones I and II could be explained as a competition between the changes in the order degree and the enhancing of the vacancies mobility, revealed by the exothermal reaction with peak at 650 K in Figure 1. In fact, the increase in Bm and the almost constant Hc behaviour in zone I can be related to the enhanced mobility of vacancies related to their recovery, in agreement with the results for Fe-10at.% Si. The subsequent decrease in Bm and increase in Hc in zone II could be related to the increase in the D0<sub>3</sub> order contribution. Finally the increase in Bm and the decrease in Hc, exhibited in zone III can be related to the recovery of quenched-in-defects, as a consequence of the D0<sub>3</sub> → bcc transition, which is revealed by the increase in the mobility of defects viewed through the higher values of damping in the region of lower temperatures (see Figure 6).



Figure 10 shows the behaviour of  $B_m$  and  $H_c$  for the ternary Fe-4at.% Al-8at.% Ge, where both behaviours are again not monotonous as a function of the annealing temperature, giving rise to three different stages. The decrease in  $B_m$  and increase of  $H_c$  in zone I (Figure 10) can be related to the decrease in the dislocations mobility by a pinning processes which through a magnetostrictive coupling diminishes the domain walls mobility. In zone II, where the improvement of the magnetic quality of the alloys starts, can be related to the increase in the mobility of point and linear defects, since the development of the GB is starting. Finally, the subsequent improvement of the magnetic quality in zone III can be related to an increase in the mobility of the domain walls due to a further recovery of the microstructure which gives rise to an enhanced mobility of defects, owing to the decrease in the amount of quenched-in defects.

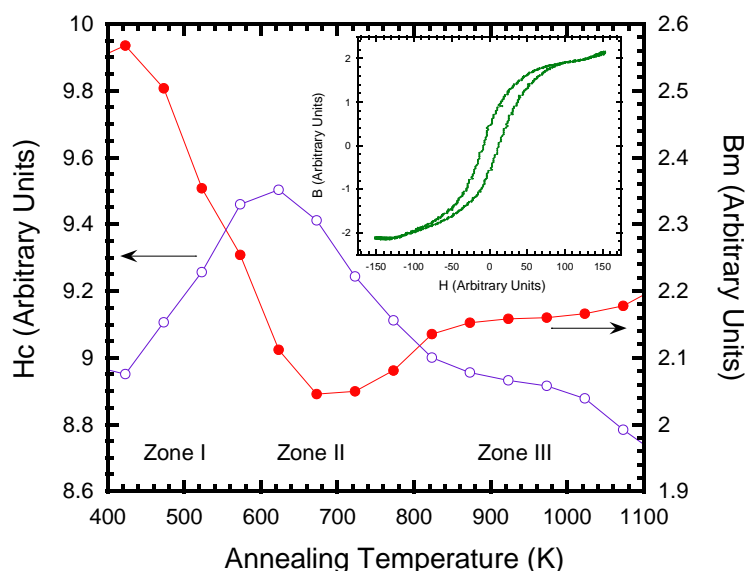


**Figure 10:**  $B_m$  and  $H_c$  as a function of annealing temperature for Fe-4at.% Al-8at.% Ge. Being magnetic loops traced at room temperature. Inset shows a hysteresis loop.

#### 4. CONCLUSIONS

The influence of both the microstructural state and the type of order, and its changes, as a function of temperature on the magnetic properties in several Fe-based alloys has been determined. The microstructure has been characterized by means of differential thermal analysis, mechanical spectroscopy and neutron thermodiffraction studies, and the results were correlated to the magnetic properties.

The increase of order degree leads to a decrease in the mobility of the domain walls through a magnetostrictive effect, promoting a deleterious effect in the magnetic quality of the alloys.

It has been found that the B2 order has a less influence on the deterioration of the magnetic properties than  $D0_3$  order. In Fe-10at.% Si, the magnetic properties improve always with an increase in the annealing temperature. In contrast, in Fe-6at.% Al-9at.% Si, it depends on the annealing temperature interval. There is a deterioration of the magnetic properties in the interval from 600 to 700 K. For Fe-4at.% Al-8at.% Ge there appears a first zone where the magnetic properties does not improve due to the pinning of dislocations. At temperatures above 650 K, an improvement in the magnetic behaviour develops due to the recovery and the annihilation of quenched-in-defects and -dislocations.

#### 5. ACKNOWLEDGEMENTS

Authors wants to thanks to Institute Laue Langeving (ILL), Grenoble France for the allocated neutron beantime (exp. CRG-1121) and NKK Corp and Prof I. S. Golovin for supplying Iron Silicon and ternary alloys respectively. This work was partially supported by CONICET, PIP 0179, PID-UNR; ING 450 and 453 and the Cooperation agreement between the UPNA and UNR Res. 3247/2015.

#### 6. BIBLIOGRAPHY

[1] FIORILLO, F., *Measurement and characterization of magnetic materials*, Amsterdam, Elsevier, 2004.

- [2] BOZORTH, R.M., *Ferromagnetism*, Princeton, D. Van Nostrand Company Inc, 1964.
- [3] CULLITY, B.D., *Introduction to magnetic materials*, Reading, Addison-Wesley, 1972.
- [4] FITZGERALD, A.E., KINGSLEY, C., UMANS, S., *Electric machinery*, New York, McGraw-Hill Book Company, 1983.
- [5] LAMBRI, O.A., "A review on the problem of measuring non-linear damping and the obtainment of intrinsic damping", in: Martinez-Mardones J., Walgraef D., Worner C.H. (Eds.), *Materials Instabilities*, World Scientific, pp. 249–280, 2000.
- [6] LAMBRI, O.A., PEREZ-LANDEZABAL, J.I., CANO, J.A., RECARTE, V., "Mechanical spectroscopy in commercial Fe-6 wt.% Si alloys between 400 and 1000 K", *Mater. Sci. Eng. A*, V. 370 pp. 459–463, March 2004.
- [7] FRANK, W., SEEGER, A., WELLER, M., "Interpretation of positron annihilation experiments on electron-irradiated  $\alpha$ -iron in terms of self-interstitial migration in stage III.", in: Robinson M.T., Young F.W. Jr. (Eds.), *Fundamentals Aspects of Radiation Damage in Metals*, US ERDA CONF-751006, Oak Ridge, 1976.
- [8] ELDRUP, M., "Application of the positron annihilation technique in studies of defects in solids", in: Chadwick, A.V., Terenzi, M., *Defects in Solids*, New York, NATO ASI Series, 1985.
- [9] WELLER, M., DIEHL, J., TRIFTSHÄUSER, W., "Investigations of neutron irradiated iron by positron annihilation and correlated internal friction measurements", *Solid State Commun.*, V. 17, pp. 1223–1226, Nov. 1975.
- [10] HUMPHREYS, F.J., HATHERLY, M., *Recrystallization and related annealing phenomena*, Netherlands, Pergamon, 2002.
- [11] LAMBRI, O.A., BULEJES, E.D., GORRIA, P., TINIVELLA, R.J., "Mechanical spectroscopy study in commercial grain oriented silicon steel", *J. Mater. Sci.*, V.35, pp. 79–85, Jan. 2000.
- [12] LAMBRI, O.A., PEREZ-LANDEZABAL, J.I., CUELLO, G.J., CANO, J.A., RECARTE, V., SIEMERS, C., GOLOVIN, I.S., "Mechanical spectroscopy in Fe-Al-Si alloys at elevated temperatures", *J. Alloys Compd.*, V. 468, pp. 96–102, Dec. 2009.
- [13] MIYAZAKI, T., KOZAKAI, T., TSUZUKI, T., "Phase decompositions of Fe-Si-Al ordered alloys", *J. Mater. Sci.*, V. 21, pp. 2557–2564, July 1986.
- [14] PAVLOVA, T.S., GOLOVIN, I.S., SINNING, H.R., GOLOVIN, S.A., SIEMERS C., "Internal friction in Fe-Al-Si alloys at elevated temperatures", *Intermetallics*, V. 14, pp. 1238–1244, Oct. 2006.
- [15] LAMBRI, O.A., PÉREZ-LANDEZÁBAL, J.I., GARGICEVICH, D., RECARTE, V., BONIFACICH, F.G., CUELLO, G.J., SÁNCHEZ-ALARCOS, V., "Order evolution in Iron-based alloys viewed through amplitude dependent damping studies", *Mater. Trans.*, V. 56, pp. 182–186, Jan 2015.
- [16] MOLINAS, B.J., POVOLO, F., "Present state of the controversy about grain boundary relaxation", *Nuovo Cim.*, V. 14, pp. 287–332, March 1992.
- [17] LAMBRI, O.A., PÉREZ-LANDEZÁBAL, J.I., CUELLO, G.J., GARGICEVICH, D., RECARTE, V., BONIFACICH, F.G., GIORDANO, E.D., SANCHES-ALARCOS, V., "Relation between order degree, damping behaviour and magnetic response in Fe-Si and Fe-Al-Si alloys", *Neutron News*, V. 25, pp. 28–31, Oct. 2014.
- [18] GARGICEVICH, D., LAMBRI, O.A., PÉREZ-LANDEZÁBAL, J.I., RECARTE, V., BONIFACICH, F.G., CUELLO, G.J., SÁNCHEZ-ALARCOS, V., "Mobility of dislocations and grain boundaries controlled by the order degree in iron-based alloys", *J. Phys. Conf. Ser.*, V. 663, pp. 12013, Dec. 2015.
- [19] CAHN, R.W., HAASEN, P., *Physical Metallurgy 3rd edition*, Amsterdam, North Holland Physics Publishing, 1983.
- [20] VIALA, B., DEGAUQUE, J., BARICCO, M., FERRARA, E., PASQUALE, M., FIORILLO, F., "Magnetic and mechanical properties of rapidly solidified Fe-Si 6.5 wt% alloys and their interpretation", *J. Magn. Magn. Mater.*, V. 160, pp. 315–317, 1996.
- [21] VIALA B., DEGAUQUE, J., FAGOT, M., BARICCO, M., FERRARA, E., FIORILLO, F., "Study of the brittle behaviour of annealed Fe-6.5 wt%Si ribbons produced by planar flow casting", *Mater. Sci. Eng. A*, V. 212, pp. 62–68, 1996.